nature neuroscience



# Dynamic shifts in the owl's auditory space map predict moving sound location

Ilana B Witten[1,2], Joseph F Bergan[1,2] & Eric I Knudsen[1]

**The optic tectum of the barn owl contains a map of auditory space. We found that, in response to moving sounds, the locations of receptive fields that make up the map shifted toward the approaching sound. The magnitude of the receptive field shifts increased systematically with increasing stimulus velocity and, therefore, was appropriate to compensate for sensory and motor delays inherent to auditory orienting behavior. Thus, the auditory space map is not static, but shifts adaptively and dynamically in response to stimulus motion. We provide a computational model to account for these results. Because the model derives predictive responses from processes that are known to occur commonly in neural networks, we hypothesize that analogous predictive responses will be found to exist widely in the central nervous system. This hypothesis is consistent with perceptions of stimulus motion in humans for many sensory parameters.**

Predicting the future state of the world is essential for generating adaptive behavior. For example, to orient the eyes toward a moving stimulus, an animal must predict the future position of the stimulus in order to compensate for the substantial delays between sensation and motor output. Without such prediction, an animal would orient to a position in space that lags behind the stimulus' true position. Here we describe a neural circuit in the barn owl's optic tectum (homolog of the mammalian superior colliculus) that makes such a prediction in response to the motion of an auditory stimulus.

Motion has systematic effects on space-dependent response properties, even in populations of neurons that are not tuned for the direction of motion. In the retina, moving bars of light can cause the spatial distribution of neural activity to shift, and the direction of the shift is appropriate to compensate for sensory delays[1]. However, the magnitude of the shift does not increase with stimulus speed, even though a larger shift is needed for the prediction to be adaptive at higher speeds.

In addition, stimulus motion has been shown to have systematic effects on auditory responses at various sites in the central auditory system. These studies have shown that the direction and speed of a moving sound changes the space-dependent response properties of neurons[2–7]. In these studies, unit responses were measured using a single stimulus that swept across the receptive field, so that responses to different spatial locations were measured at different times after stimulus onset. Because auditory spatial receptive fields can sharpen markedly after stimulus onset[8], not controlling for time after stimulus onset confounds onset-dependent receptive field sharpening with shifts in receptive field location. To resolve the effects of sound motion on receptive field size and location, separately, requires that both receptive field edges be measured at identical time points following stimulus onset. Only a shift in receptive field location could aid in predicting the future locations of moving stimuli.

Here, we describe a new stimulus protocol for measuring the effect of motion on receptive field size and location and demonstrate that auditory receptive fields in the owl's optic tectum shift substantially following the onset of a moving sound. Moreover, the time course over which receptive field shifts develop is behaviorally relevant and the magnitude of these shifts is appropriate for guiding adaptive behavior.

The optic tectum is a midbrain structure that participates in orienting the owl's gaze toward auditory stimuli[9]. The auditory system derives stimulus location by analyzing various monaural and binaural cues. The primary cue for the horizontal position (azimuth) of a sound source is interaural time difference (ITD), caused by the delay between sound reaching the near versus the far ear[10]. The primary cue for the vertical position (elevation) is interaural level difference (ILD) for high frequency components ($>4$ kHz), caused by a physical asymmetry of the owl's external ears[11,12]. Neurons in the owl's optic tectum are sharply tuned for both ITD and ILD, and are organized according to the cue values to which they are tuned, forming a topographic map of auditory space[13].

To test the effect of stimulus motion on auditory spatial tuning, we presented sounds through earphones (dichotically) and simulated stimulus motion in azimuth with continuous changes in ITD cues. Presenting sounds dichotically allowed us to randomly interleave virtual motion sweeps of different velocities and across different portions of space. Motion in azimuth is readily mimicked in a quantitative and compelling manner because, across a large portion of frontal space, ITDs vary linearly with azimuth and are consistent across frequencies[14,15]; indeed, sounds presented dichotically with a constant ITD elicit predictable azimuthal head turns in behaving

[1]Department of Neurobiology, Stanford University Medical School, Stanford, California 94305, USA. [2]These authors contributed equally to this work. Correspondence should be addressed to E.I.K. (eknudsen@stanford.edu).

Received 6 July; accepted 12 September; published online 1 October 2006; doi:10.1038/nn1781

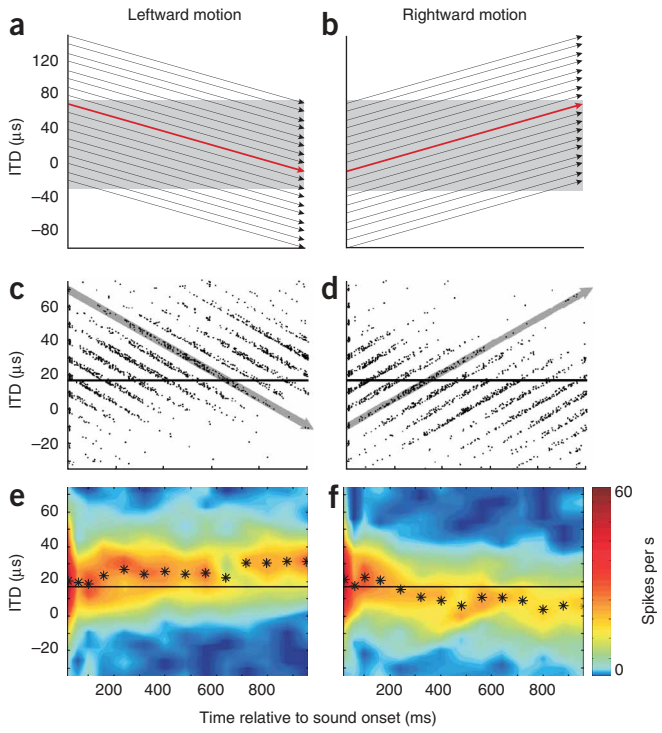


**Figure 1** Predictive shifts in spatiotemporal receptive fields in response to stimulus motion (80 μs ITD per s) for a single optic tectum unit. (**a**–**f**) Left column, leftward motion; right column, rightward motion. Horizontal black lines in **c**–**f** indicate the best ITD measured with stationary stimuli. (**a**,**b**) Each arrow represents a single moving auditory stimulus. Each stimulus was presented one at a time in a randomly interleaved fashion. The shaded region indicates the portion of the measured spatiotemporal receptive field that is plotted in subsequent panels. (**c**,**d**) Raster plots showing the responses to the set of moving auditory stimuli. Gray diagonal arrows indicate the stimulus trajectories shown as red arrows in **a** and **b**. Points overlaid on each arrow represent spikes that occurred, for each of 25 repetitions, at the corresponding spatial and temporal positions of the stimulus. Points plotted on other diagonals represent the responses to stimuli beginning at other ITDs. (**e**,**f**) Contour plots of responses shown in **c** and **d**. Asterisks indicate the best ITD value for each time bin.

owls[10]. In contrast, quantitative simulation of stimulus motion in elevation is complicated because ILD values vary nonmonotonically with both elevation and azimuth and are highly frequency dependent[14,15]. Hence, our analysis was restricted to the effects of simulated motion in azimuth. Therefore, whenever we use the term 'space' in this paper, we are referring exclusively to azimuth. However, because elevation, like azimuth, is represented topographically in the optic tectum, we hypothesize that similar effects would be observed for both dimensions.

## RESULTS

### Moving sounds cause predictive RF shifts

We presented randomly interleaved, virtual motion sweeps that began at evenly spaced ITD values spanning the receptive field of the recording site (**Fig. 1a**,**b**). The sounds, which swept either to the left or to the right, were presented one at a time. By compiling the responses to the stimulus sweeps, we could construct a neuron's spatial receptive field to moving stimuli for any time point following sound onset—that is, a neuron's spatiotemporal receptive field to moving stimuli. This analysis demonstrated both a sharpening of receptive fields over time following stimulus onset, as well as predictive shifts in receptive field locations. These data allowed us to quantify the time course of the effects of motion on receptive field structure, and to relate such changes to behavior.

The spatiotemporal receptive field of a single optic tectum unit was measured in response to simulated motion at a speed of 80 μs ITD per s, or ~32° per s (**Fig. 1c–f**; for barn owls, 2.5 μs ITD ≈ 1°, ref. 16). Responses to each ITD sweep (**Fig. 1c**,**d**, diagonals) increased as the stimulus entered the unit's receptive field. The average responses to all stimuli was calculated as a function of ITD and time relative to sound onset (**Fig. 1e**,**f**). Near sound onset, the receptive field was relatively broad and centered on 17 μs ITD with the right ear leading (~7° right). Within 100 ms of sound onset, the receptive field had sharpened markedly and, by 300 ms, the receptive field had shifted toward more right ear leading ITDs for leftward motion (**Fig. 1e**, asterisks) and toward more left ear leading ITDs for rightward motion (**Fig. 1f**, asterisks). By the last 200 ms of the stimulus, leftward motion had induced a 14 ± 1.5 μs shift (mean ± s.e.m.; ~6°) and rightward motion had induced a 12 ± 1.9 μs shift (~5°) in the weighted average of the responses (best ITD; Methods) relative to the best ITD for the receptive field measured in response to stationary stimuli (horizontal black line). The dynamically shifted best ITDs for leftward and rightward motion, measured from responses 800–1,000 ms after sound onset, were each significantly different from the best ITDs measured for interleaved, 200-ms-long stationary stimuli ($P < 0.0001$, two-tailed $t$-test).

The average receptive field shifts induced across the entire population of sampled sites ($n = 17$) was measured in response to a speed of 80 μs ITD per s (~32° per s; **Fig. 2**). The shifts developed rapidly over the first several hundred milliseconds (exponential fit, time

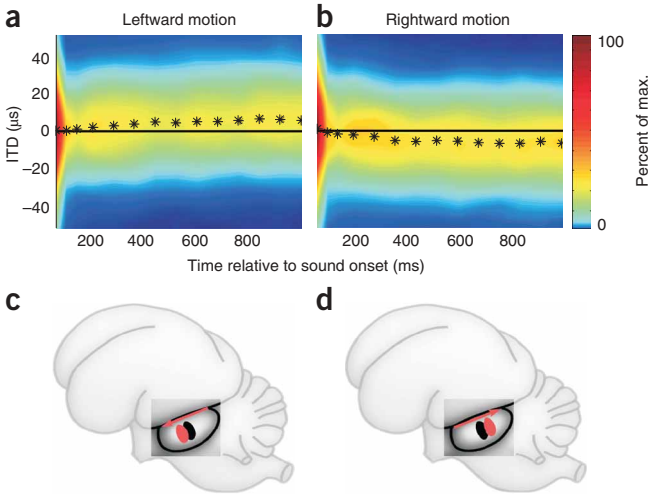


**Figure 2** Predictive shifts in spatiotemporal receptive fields in response to stimulus motion for the population. (**a**,**b**) Average responses for all sites to moving auditory stimuli (80 μs ITD per s). Individual receptive fields were normalized and centered (0 μs ITD) relative to the best ITD measured with stationary stimuli (horizontal lines). (**c**,**d**) Schematic illustration of the effect of stimulus motion on the distribution of auditory responses across the neural map of space in the optic tectum. Black ovals represent the area of optic tectum activated by a stationary sound and red ovals represent the area of optic tectum activated by a moving sound at the same location. Arrows indicate the direction of stimulus motion across the neural representation of space.

constant = 260 ms). The magnitudes of the final shifts were 7 ± 1 μs (~3°) for both leftward and rightward motion (**Fig. 2a**,**b**, asterisks). For motion of 80 μs ITD per s, best ITD values shifted in the predictive direction for every site tested (measured from 800–1,000 ms after sound onset). The best ITDs to leftward motion were significantly different from the best ITDs to rightward motion for 14 of the 17 individual sites (measured from 800–1,000 ms after sound onset; $P < 0.05$, two-tailed $t$-test). For the population, best ITDs for rightward and leftward motion (measured from 800–1,000 ms after sound onset) were each significantly different from the best ITDs measured for 200-ms-long stationary stimuli ($P < 0.0001$, paired two-tailed $t$-test).

The predictive shifts in receptive fields could be mediated by a change in either of the receptive field borders: the border that the stimulus approached first (leading edge) or the border at which the stimulus exited the receptive field (lagging edge). In fact, we found that both edges shifted significantly in the predictive direction (**Fig. 3**; $P < 0.0005$, two-tailed $t$-test). Thus, overall receptive field shape and the extent of the population response in the optic tectum were maintained in response to motion.

Because space is represented topographically in the optic tectum, the population receptive field (**Fig. 2a**,**b**) can be used to infer the average distribution of neural activity across the optic tectum space map, as a function of time, in response to a moving sound. The region of the tectal map that responded to stationary stimuli of a given ITD value (**Fig. 2c**,**d**, black oval) was different from the region that responded to moving stimuli of the same ITD value (**Fig. 2c**,**d**, red oval). The optic tectum encodes gaze changes as a topographic motor map that is aligned with the auditory map measured with stationary stimuli[17]. Assuming that this motor map remains constant, the motion-induced shift in auditory responses across the optic tectum encodes a gaze change to the future location of a moving auditory stimulus.

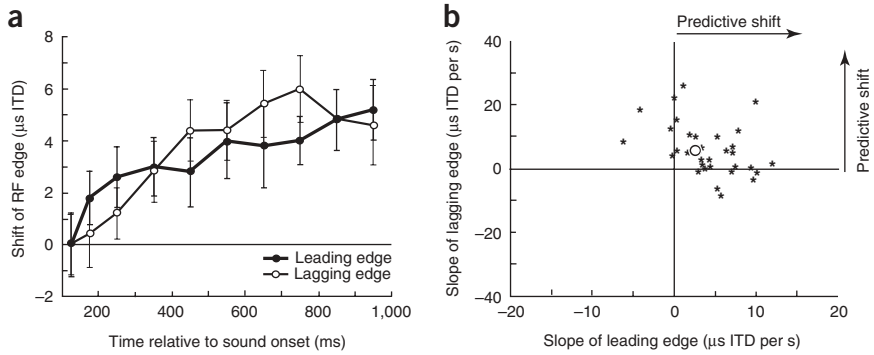


**Figure 3** Predictive shifts of the leading and lagging edges of the receptive field measured at 80 μs ITD per s. (**a**) Average shift in the two receptive field edges. At each time bin, edges are defined as the ITD value that generates 50% of the maximum response of the final time bin. Error bars are bootstrap s.e.m (**b**) Shift of leading versus lagging edge during the final 900 ms of the stimulus (slope of a line fit to each edge as a function of time). Positive values indicate shifts in the predictive direction. Black asterisks are the shifts of edges for all optic tectum sites. The white dot indicates the shift resulting from the computational model with the same parameters as in **Figure 5b**.

## Receptive field shifts compensate for sensorimotor delays

In order for neuronal activity in the optic tectum to predict sound source location at some future time, the magnitude of receptive field shifts must increase with stimulus speed. This was found to be the case. We defined receptive field shifts as half the difference between the best ITDs for rightward and leftward motion (**Fig. 4a**). At sound onset, receptive field shifts lagged behind the stimulus, as evidenced by the negative difference between leftward and rightward best ITDs. This lag was due to the ~8 ms auditory response latency of the optic tectum units. Leftward and rightward best ITDs were identical (**Fig. 4a**, dashed line) only after unit tuning had shifted enough to compensate for response latency, which had occurred for all stimulus speeds by 200 ms after sound onset. Increasing stimulus speeds caused systematic increases in the magnitude of the final shifts (measured 800–1,000 ms after sound onset; $P < 0.0001$, one-way analysis of variance (ANOVA)).

The receptive field shifts demonstrated here were of the appropriate direction and magnitude to generate adaptive behavior. We calculated the time-lead that corresponded to a particular receptive field shift by dividing the difference between the best ITDs measured for moving and stationary stimuli by the speed of the moving stimulus. Predictive time-leads ranged from 87 ms to 144 ms for the speeds tested (**Fig. 4b**). Time-leads greater than zero indicate that the receptive field shifts compensated beyond the sensory response delays. The time-leads matched the motor delays for the circuit, as saccadic gaze changes evoked by electrical microstimulation of the owl's optic tectum are completed in approximately 100 ms (ref. 17). Thus, the shifts were large enough to compensate for motor as well as sensory delays for all speeds tested.

Our results demonstrate that the representation of a moving auditory stimulus in the optic tectum shifts dynamically, and compensates adaptively for the direction and speed of stimulus motion. Immediately following

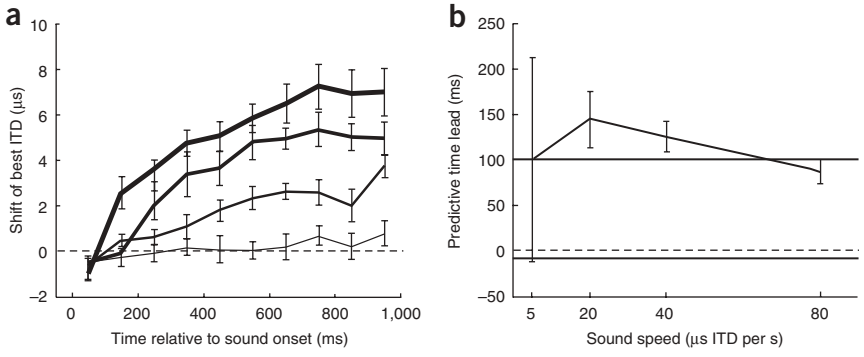


**Figure 4** Receptive field shifts increase with stimulus velocity. (**a**) Predictive shift, averaged across the population, as a function of time relative to sound onset, for speeds of 5, 20, 40 and 80 μs ITD per s (thicker lines correspond to faster speeds). The predictive shift is defined as one-half the difference between the best ITD values measured with leftward versus rightward motion. The dashed line indicates no difference in best ITDs, whereas positive values indicate predictive shifts of best ITD. (**b**) Predictive time-leads for all speeds tested. The horizontal line at 100 ms indicates the time-lead appropriate for orienting movements. The horizontal line at –8 ms indicates the time-lag expected due to the auditory response delays. All points represent the average predictive shift in best ITD from the last 200 ms of panel **a** divided by the stimulus speed. Error bars are bootstrap s.e.m. for both **a** and **b**.

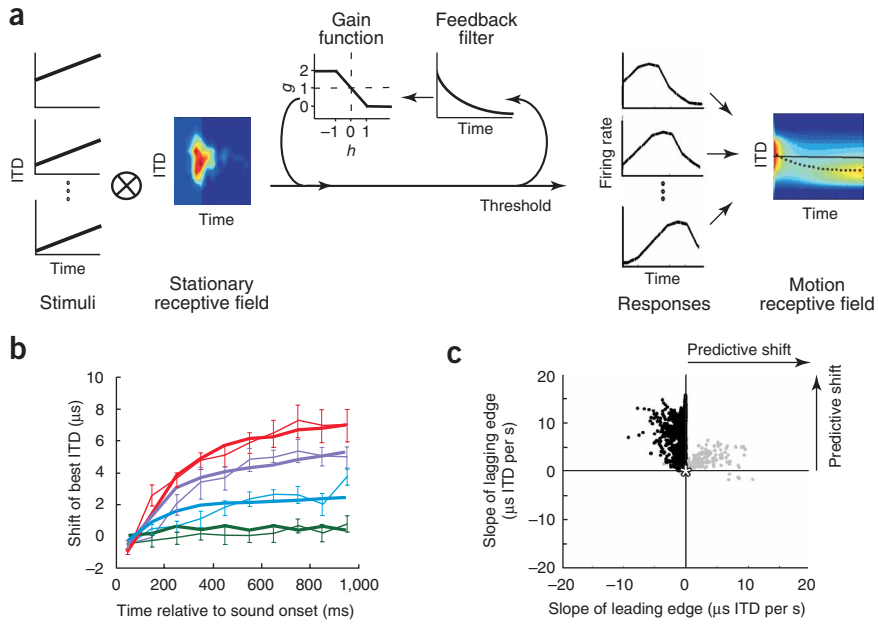


**Figure 5** Computational model reproduces receptive field shifts. (**a**) A model that accounts for predictive shifts of auditory tuning curves in response to motion. Moving auditory stimuli were convolved with a sample receptive field measured with stationary stimuli (stationary receptive field) and multiplied by a gain factor ($g$) to obtain a response. The gain factor was calculated by filtering the responses with an exponential (feedback filter) and inputting the filtered response ($h$) into the gain function. The response was then thresholded. Finally, the responses to all sound sweeps were combined to obtain the spatiotemporal receptive field to the moving stimuli (motion receptive field). The horizontal line indicates best ITD for stationary stimuli. The asterisks indicate best ITDs as a function of time for moving stimuli. (**b**) Shift in best ITD as a function of time relative to stimulus onset, for the data (from **Fig. 4a**; thin lines) and the model (thick lines). Speeds: 5 (green), 20 (blue), 40 (purple) and 80 (red) μs ITD per s. ($\tau = 250$ ms; $I = -0.05 \times \max(R_e(x,t))$; $B = 210$ per s; $\theta = 0$) (**c**) Shift of leading versus lagging edges, quantified in the same manner as in **Figure 3b**, for the computational model over a wide range of parameter values ($\tau = 150$ to 350 ms; $B = 20$ to 700 per s; $\theta = \min(f)$ to $\max(f)$). Gray dots, feedback with an inhibitory surround ($I = -0.05 \times \max(R_e)$); black dots, feedback without an inhibitory surround ($I = 0$); Asterisk, no feedback ($B = 0$).

sound onset, stimulus location is represented relatively broadly in the space map. Within 100 ms of sound onset, the representation sharpens markedly and the motion of the stimulus causes the representation to begin shifting in the predictive direction. By 500 ms after sound onset, the representation has become centered at a location in the map that predicts where the stimulus source will be approximately 100 ms later.

### Computational model simulates receptive field shifts

To identify potential mechanisms that could account for motion-induced dynamic receptive field shifts, we constructed a model for computing optic tectum responses that was sensitive to stimulus motion (**Fig. 5a**). The model was based on a similar model for the retina[1]. The sensitivity of the model to the direction of stimulus motion was accomplished by having past responses modify future responses through negative feedback: strong responses decreased the subsequent gain of neural responses and weak responses increased the subsequent gain. The gain was calculated by filtering responses with an exponential, and then inputting the filtered responses ($h$) into a gain function ($g(h)$). The gain function had a negative slope at the origin, creating an inverse relationship between the strength of previous responses and the gain of responses during the subsequent time step. This model replicated the magnitude, time course and speed dependence of the receptive field shifts (**Fig. 5b**).

Negative feedback was essential to yield predictive shifts of both the lagging and leading edges of the receptive fields. As the sound crossed the excitatory receptive field, responses became stronger (increased $h$), causing the gain ($g$) to decrease because of the negative slope of the gain function (**Fig. 5a**). This decrease in gain resulted in a lower firing rate by the time the sound reached the lagging edge, causing the lagging edge to shift toward the approaching sound. Such negative feedback on excitatory drive would correspond to response adaptation, for example. However, a decrease in gain caused by strong responses also caused the leading edge of the receptive field to shift in the nonpredictive direction (**Fig. 5c**, black dots), indicating that an additional element was needed to fully explain the data.

Adaptive shifts in the leading edge were accomplished by adding an inhibitory surround to the stationary receptive field. As a sound crossed the inhibitory surround and approached the excitatory receptive field, inhibition suppressed responses (decreased $h$), thereby causing an increase in the gain $g$ because of the negative slope of the gain function (**Fig. 5a**). By the time the sound reached the leading edge of the receptive field, the gain was large, thereby advancing the leading edge in the predictive direction. This increase in gain caused by inhibition would correspond to postinhibitory rebound, for example. By adding an inhibitory surround to the excitatory receptive field, we were able to replicate the predictive shifts that occurred at both edges (**Fig. 5c**, gray dots). As expected, neither receptive field edge shifted without feedback (**Fig. 5c**; asterisk).

The model indicated that negative feedback is needed to simulate predictive receptive field shifts in the optic tectum: there must be a decrease in unit responsiveness following excitation and an increase in unit responsiveness following inhibition. These mechanisms should also shape unit responses to sequential, stationary stimuli that originate from different locations in a unit's receptive field. We examined this prediction quantitatively, and compared the results with unit responses recorded in the optic tectum. For both the model and the data, we first presented a 250-ms-long priming sound either at the receptive field's excitatory center (best ITD; **Fig. 6a,b**, white arrowheads) or in the inhibitory surround (best ITD + 60 μs; **Fig. 6a,b**, black arrowheads). The second 250-ms-long test stimulus was presented from locations that spanned the receptive field.

The model produced a decrease in responsiveness to the stationary test stimulus when it was presented immediately after the excitatory priming stimulus (**Fig. 6a**, white circles). Conversely, the model produced an increase in responsiveness to a stationary test stimulus when it was presented immediately after the inhibitory stimulus (**Fig. 6a**, black circles). The predictions of the model were tested experimentally at a subset of optic tectum sites ($n = 19$). The experimental data followed the predictions of the model: unit responsiveness decreased following an excitatory stimulus (**Fig. 6b**, white

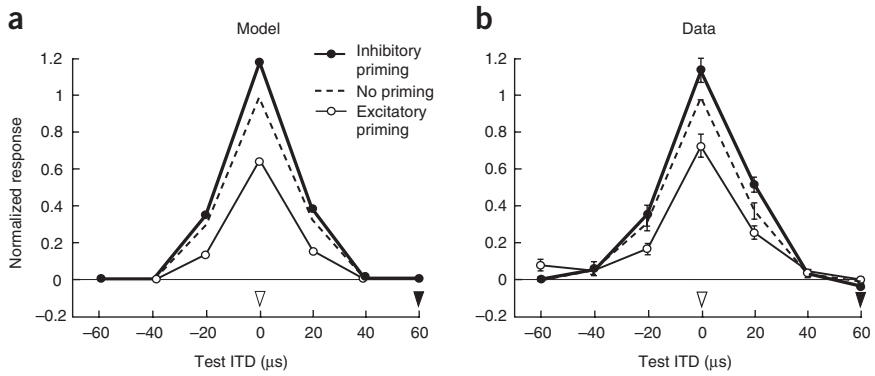


**Figure 6** Effects of an excitatory or inhibitory priming stimulus on responses to a subsequent test stimulus. (**a**) Predictions of the model. (**b**) Population average for experimental data from the optic tectum ($n = 19$ sites). Both the priming and the test stimuli were 250-ms-long noise bursts. White arrowheads indicate the ITD of the excitatory priming stimulus; black arrowheads indicate the ITD of the inhibitory priming stimulus. The curves indicate the average responses during the subsequent test stimulus. White circles (○) are responses to stimuli following the excitatory priming stimulus; black circles (●) are responses to stimuli following the inhibitory priming stimulus. Dashed lines are responses to the test stimulus alone. In **a** and **b**, responses were normalized by the maximum firing rate in response to the test stimulus alone. In **b**, data were aligned relative to the best ITD for each site (indicated as 0 μs ITD); error bars represent bootstrap s.e.m.

circles; two-tailed $t$-test, $P < 0.0001$) and increased following an inhibitory stimulus (**Fig. 6b**, black circles; two-tailed $t$-test, $P = 0.04$).

## DISCUSSION

Stimulus motion affects auditory responses in several neural circuits. A number of studies in the inferior colliculus of gerbils, guinea pigs and bats have demonstrated that neural response patterns change with stimulus motion and that responses to particular values of auditory spatial cues depend on the recent history of stimulation[2,3,5,6]. Consistent with our conclusions, these effects have been attributed to adaptation and postinhibitory rebound[6,18,19]. However, in these studies the effect of motion was measured with a single stimulus that swept across the receptive field. Such a stimulus could not assess the effects of motion on both receptive field edges at the same times after stimulus onset. Therefore, although these studies show that receptive fields change in response to motion, the data could not distinguish between a sharpening and a shifting of the receptive fields.

By using a stimulus protocol that measured the entire receptive field at equivalent times after stimulus onset, we demonstrated that auditory receptive fields in the optic tectum space map both sharpen and shift following the onset of a moving stimulus. Thus, this is the first unequivocal demonstration that auditory receptive fields shift predictively in response to stimulus motion.

Moreover, detailed knowledge of the function and functional organization of the optic tectum allows us to interpret quantitatively the adaptive value of the motion-induced shifts in receptive field location. Because space is represented topographically in the optic tectum[20], we can infer the effect of stimulus motion on the distribution of neural activity across the optic tectum from the effects of motion on the receptive fields of single units (**Fig. 2c,d**). In addition, the behavioral significance of the distribution of activity in the optic tectum is known: the locus of activity encodes changes in gaze direction[17]. These gaze changes are carried out by saccadic movements of the eyes and head, at latencies and for durations that have been measured.

The motion-induced shifts in receptive field location scale nearly linearly with velocity across the entire range tested and, in this manner, predict the location of a moving sound ~100 ms in the future. This is approximately the time required for an owl to acquire an auditory target with its gaze[17]. It is likely that these predictive receptive field shifts represent shifts occurring, at least partially, at earlier stages in the auditory pathway, particularly in the external nucleus of the inferior colliculus (ICX) where the auditory map of space is created[21]. By the level of the optic tectum, the match between the magnitude of the receptive field shifts in the optic tectum and the shifts needed to execute adaptive behavior is remarkable. To allow these receptive field shifts to develop completely, owls would need to listen to a moving sound for at least 500 ms before programming an orienting response to a stimulus (**Fig. 4a**). Although owls can respond with shorter latencies (<100 ms) to sounds[22], they often do not, especially when more than one stimulus is present in the environment. When an owl does respond to a moving sound with a latency of less than 500 ms, it should underestimate the required compensation.

Our computational model indicates that the responses of optic tectum neurons must be shaped by negative feedback such that a decrease in responsiveness follows excitation and an increase in responsiveness follows inhibition. These phenomena have been demonstrated previously in the auditory space map of the ICX, which drives auditory responses in the optic tectum[23]. ICX neurons adapt strongly after being driven by an excitatory stimulus[24]. The receptive fields of ICX neurons include extensive inhibitory surrounds[25], and many ICX units exhibit rebound excitation following stimulation of the inhibitory surround[8]. In addition, we demonstrated directly that both kinds of negative feedback shape responses in the owl's optic tectum (**Fig. 6b**).

The predictive receptive field shifts we observed would occur in response either to the motion of a stimulus relative to the owl (stimulus motion) or to the motion of the owl relative to a stimulus (self-induced motion). It is unlikely that owls experience stimulus motion with speeds much above 10° per s (perpendicular translation of 20 cm $s^{-1}$ at a distance of 1 m). While hunting, however, they might experience high speeds of self-induced motion as they fly past an acoustic stimulus that is offset from the owl's direction of flight. Indeed, the predictive shifts of the optic tectum map may be particularly valuable for making corrective saccades to acoustic stimuli as the owl approaches its target.

The receptive field shifts observed in this study bear striking resemblance to motion-induced perceptual effects that have been reported in humans for a number of stimulus features. For instance, sound motion shifts our perception of sound location ahead of the true location of the source[26]. Like the receptive field shifts observed in this study, which develop over several hundred milliseconds, the perceived location of a moving stimulus is biased more by a 300-ms-long sound than by a shorter sound. As with our neural recordings, the magnitude of the perceptual effect increases with stimulus velocity. Similar motion-induced perceptual effects have been observed for a wide variety of stimulus parameters, including location and frequency in the auditory domain[27], and luminance, color and spatial frequency in the visual domain[28,29]. As demonstrated by our model, motion-dependent receptive field shifts can occur in mapped representations

as a result of common neural properties such as adaptation and rebound from lateral inhibition, without the involvement of specialized motion detectors. Therefore, to the degree that a sensory parameter is processed by neural circuits that possess these common properties, the results described here for the optic tectum indicate that motion will induce predictive shifts in the representations of these parameters throughout the central nervous system.

## METHODS

**Animals.** Twelve adult barn owls were pair-housed in flight aviaries. Birds were cared for in accordance with the US National Institutes of Health Guide for the Care and Use of Laboratory Animals and the Stanford University Institutional Animal Care and Use Committee.

**Electrophysiological recordings.** Owls were anesthetized with 1% halothane mixed with nitrous oxide and oxygen (45:55), and a small stainless steel fastener was attached to the rear of the skull with dental acrylic. Craniotomies were opened dorsal to the optic tectum, based on stereotaxic coordinates.

During recording sessions, owls were suspended in a prone position with the head stabilized using the mounted fastener. Nitrous oxide and oxygen (45:55) were administered continuously.

Multiunit and single-unit responses were isolated from the deep layers (11–13) of the optic tectum with insulated tungsten microelectrodes (6–13 MΩ at 1 kHz). The layers were identified on the basis of their firing properties, as confirmed previously[30]. Using a constantly moving search stimulus, we searched within these layers for neurons that exhibited sustained firing to stimuli within their receptive fields. Units were sampled from the portion of the optic tectum that represented frontal space (within 20° of the visual axes). A total of 19, 11, 10 and 17 single-unit or multiunit sites were measured for speeds of 5, 20, 40, and 80 μs ITD per s, respectively. In addition, 19 multiunit sites were recorded in tests for adaptation and postinhibitory rebound with stationary stimuli. Spike times and waveforms were stored using TDT hardware (RA-16) controlled by customized MATLAB (Mathworks) software.

**Stimuli.** Auditory responses were assessed by presenting frozen broadband noise bursts (flat amplitude spectrum ± 1 dB; 2–10 kHz; 20–30 dB above threshold) dichotically through earphones placed 5 mm from the tympanic membrane. The noise waveform presented to each ear was the same, except for a difference in the relative timing that corresponded to the ITD. In this study, negative ITDs indicate left ear leading sounds and positive ITDs indicate right ear leading sounds. For both stationary and moving stimuli, ITDs were generated using the ShortDynDel function running on TDT hardware (RP2). At every sampled time point, this function interpolates between the current and the previous signal value using the function $\sin(x)/x$, and then shifts the signal by the appropriate delay. Waveforms were sampled at 50 kHz.

For virtual motion stimuli, ITD changed at a constant rate for the 1,000-ms duration of the sound (**Fig. 1a,b**, arrows). The stimuli were spaced 10 μs ITD apart and traversed all or part of the receptive field. The ITD of moving stimuli changed at speeds of 5, 20, 40 or 80 μs ITD per s, in order to simulate auditory motion at speeds of 2, 8, 16 or 32° per s, respectively. Stimulus sweeps for all speeds and both directions were randomly interleaved and were presented with 25 repetitions at an interstimulus interval of 2 s. Spike times and stimulus positions were recorded throughout each stimulus presentation.

For measuring receptive fields to stationary stimuli, 200-ms-long noise bursts with constant ITDs were presented in a randomly interleaved fashion, with ITDs spanning a 120-μs range centered on the site's best ITD. Responses to stationary noise bursts of 10 ms duration were also measured at a subset of sites to generate a stationary receptive field for use in the computational model.

In tests for adaptation and postinhibitory rebound (**Fig. 6**), we presented pairs of stationary, 250-ms-long, noise burst stimuli. A priming stimulus was delivered immediately before a test stimulus. The ITD of the priming stimulus was either at the site's best ITD, to test for adaptation, or at best ITD + 60 μs in the contralateral direction, to test for postinhibitory rebound. The subsequent test stimulus mapped out the site's responsiveness across the ITD tuning curve. Test ITDs were presented in 20-μs steps in random order. Additionally, the same test ITDs were presented in the absence of a priming stimulus. All stimulus combinations were randomly interleaved, and each stimulus was repeated 15 times.

**Data analysis and statistics.** To calculate the spatiotemporal receptive fields for stationary and moving stimuli, the response to each stimulus sweep was divided into evenly spaced time bins. We used 100-ms time bins for all statistical analyses and figures, with two exceptions. In **Figures 1e,f** and **2a,b**, the first three time bins are 40 ms and the remaining are 80 ms, so that rapidly occurring changes in the receptive field can be seen. Similarly, in **Figure 3a** the first two time bins are 50 ms, as opposed to 100 ms, so that rapidly occurring shifts in receptive field edge location can be seen. The receptive field was constructed by plotting the average firing rate as a function of the time bin and the average stimulus ITD during that time bin (**Fig. 1e,f** and **Fig. 2a,b**).

Best ITDs were calculated as the weighted average for all ITD bins yielding at least 50% of the maximum firing rate. When calculating the population receptive field (**Fig. 2a,b**) for moving stimuli, each motion receptive field was centered based on the best ITD for stationary stimuli and normalized by dividing the entire receptive field matrix by its maximum value. Then, the centered and normalized receptive fields were averaged across the population of recording sites.

All statistical tests for motion-dependent shifts of the best ITD were performed on the best ITDs from the final 200 ms (800–1,000 ms poststimulus onset for moving stimuli). This time bin was chosen because predictive receptive field shifts had stabilized by this point. For the sample site of **Figure 1**, two-tailed *t*-tests were performed to determine whether the best ITDs for leftward and rightward moving stimuli were different from the best ITD measured with stationary stimuli, from 0–200 ms after stimulus onset. Additionally, at each site, a two-tailed *t*-test was performed to determine whether the best ITDs for leftward and rightward motion were different. Finally, for the population, paired two-tailed *t*-tests determined whether the best ITDs for leftward and rightward moving stimuli were different from best ITDs measured with stationary stimuli.

To calculate the velocity dependence of the shift in ITD tuning (**Fig. 4a**), the best ITD was calculated for each 100-ms time bin. For a given site and a given velocity of motion, the average predictive shift was defined as the best ITD for leftward motion subtracted from the best ITD for rightward motion, divided by 2. For each velocity, the predictive shifts for all sites were averaged across the population to create **Figure 4**. To test whether stimulus velocity was a significant factor in determining the amount of receptive field shift, a one-way ANOVA was performed on the mean predictive shift (based on best ITDs measured 800–1,000 ms after stimulus onset) for each speed tested.

The leading and lagging receptive field edges for each time bin were defined as the ITD values that corresponded to a firing rate that was 50% of the maximum firing rate for the final time bin. In contrast to the previous analyses, to test for a shift in the edges, the first 100 ms were excluded because of the marked receptive field sharpening that occurred in this early time period (**Fig. 1**). A line was fit to the leading and lagging edges, respectively, as a function of time for each site, using a linear regression. Two-tailed *t*-tests were performed on the slopes of the fitted lines to determine whether they were significantly different from zero.

We applied two-tailed *t*-tests to determine the significance of changes in responses to the stationary test stimulus following the excitatory or inhibitory priming stimulus (**Fig. 6b**). For each kind of priming stimulus, we compared responses to the test stimulus at the best ITD with and without the priming stimulus.

**Model.** The model, which was used to predict responses to moving sounds, consisted of two main components. The first was the receptive field in response to stationary sounds. The second was a negative feedback component, which caused strong previous responses to decrease the gain of future responses and weak previous responses to increase the gain of future responses.

The stationary receptive field, $R(x,t)$, was created by summing an excitatory and an inhibitory component—that is, $R(x,t) = R_e(x,t) + R_i(x,t)$. $R_e(x,t)$, the excitatory component of the stationary receptive field, was obtained by

measuring the responses of a representative optic tectum unit to very short (10 ms) sound bursts that ranged in ITD, centered on the unit's best ITD. The excitatory field began 8 ms after sound onset, corresponding to the latency of the unit. $R_i(x,t)$, the inhibitory receptive field, was spatially uniform in strength and began 12 ms after stimulus onset. The relative timing of excitation and inhibition was chosen to be consistent with previous reports in the barn owl auditory space map[8]. The strength of the inhibitory field was determined by $I$, a free parameter in the model. The broad extent of the inhibitory field reflected the inhibitory surrounds of auditory receptive fields that have been reported in the auditory space map[25]. The parameters of the inhibitory field were the following:

$$R_i(x,t) = \begin{cases} 0 & t \leq 12 \text{ ms} \\ I & 12 \text{ ms} < t < 25 \text{ ms} \end{cases}$$

To model the response, $f(t)$, to a sweep of the sound, the moving stimulus, $S(x,t)$, was convolved with the stationary receptive field, $R(x,t)$, and multiplied by a gain function, $g(h)$.

$$f(t) = g(h) \int_{-\infty}^{\infty} dx \int_{-\infty}^{t} dt' R(x, t-t') S(x,t')$$

The gain function's input, $h$, was derived by filtering the response with an exponential ('feedback filter' in **Fig. 5a**), with time constant $\tau$ and magnitude $B$ as free parameters.

$$h(t) = \int_{-\infty}^{t} f(t') B e^{-(t-t')/\tau} dt'$$

The gain function, $g(h)$, ranged from 0 to 2, and had a negative slope at the origin, in order to create negative feedback. As the precise form of the negative feedback term in the optic tectum is unknown, we chose a piecewise linear function for simplicity.

$$g(h) = \begin{cases} 2 & h \leq -5 \\ -h/5+1 & -5 < h \leq 5 \\ 0 & h > 5 \end{cases}$$

Finally, the responses were thresholded. The threshold, $\theta$, was the final free parameter in the model.

$$T(f) = \begin{cases} \theta & f \leq \theta \\ f & f > \theta \end{cases}$$

To plot the spatiotemporal receptive field to moving sounds, multiple ITD sweeps were used to span the receptive field. Responses to the individual sweeps were combined using the same approach that was used for the experimental data.

The four free parameters in **Figure 5b** were chosen to minimize the average differences in the best ITD values between the data and the model across the four speeds.


## ACKNOWLEDGMENTS

We thank S. Baccus, R. Aldrich, A. Keuroghlian, D. Winkowski and K. Maczko for helpful comments on this paper, and P. Knudsen for technical assistance. I.B.W. and J.F.B. are recipients of National Science Foundation graduate research fellowships. J.F.B. is a recipient of a National Research Service Award. Support for the experiments came from the US National Institutes of Health.


## AUTHOR CONTRIBUTIONS

E.I.K., J.F.B. and I.B.W. conceived the experiments and wrote the paper. J.F.B. and I.B.W. performed the experiments. J.F.B. performed the data analysis and statistics. I.B.W. developed the computational model.

## COMPETING INTERESTS STATEMENT

The authors declare that they have no competing financial interests.

Published online at http://www.nature.com/natureneuroscience
Reprints and permissions information is available online at http://npg.nature.com/reprintsandpermissions/


1. Berry, M.J., II, Brivanlou, I.H., Jordan, T.A. & Meister, M. Anticipation of moving stimuli by the retina. *Nature* **398**, 334–338 (1999).
2. Ingham, N.J., Hart, H.C. & McAlpine, D. Spatial receptive fields of inferior colliculus neurons to auditory apparent motion in free field. *J. Neurophysiol.* **85**, 23–33 (2001).
3. Wilson, W.W. & O'Neill, W.E. Auditory motion induces directionally dependent receptive field shifts in inferior colliculus neurons. *J. Neurophysiol.* **79**, 2040–2062 (1998).
4. Spitzer, M.W. & Semple, M.N. Responses of inferior colliculus neurons to time-varying interaural phase disparity: effects of shifting the locus of virtual motion. *J. Neurophysiol.* **69**, 1245–1263 (1993).
5. Spitzer, M.W. & Semple, M.N. Transformation of binaural response properties in the ascending auditory pathway: influence of time-varying interaural phase disparity. *J. Neurophysiol.* **80**, 3062–3076 (1998).
6. McAlpine, D., Jiang, D., Shackleton, T.M. & Palmer, A.R. Responses of neurons in the inferior colliculus to dynamic interaural phase cues: evidence for a mechanism of binaural adaptation. *J. Neurophysiol.* **83**, 1356–1365 (2000).
7. Malone, B.J., Scott, B.H. & Semple, M.N. Context-dependent adaptive coding of interaural phase disparity in the auditory cortex of awake macaques. *J. Neurosci.* **22**, 4625–4638 (2002).
8. Wagner, H. Receptive fields of neurons in the owl's auditory brainstem change dynamically. *Eur. J. Neurosci.* **2**, 949–959 (1990).
9. Knudsen, E.I., Knudsen, P.F. & Masino, T. Parallel pathways mediating both sound localization and gaze control in the forebrain and midbrain of the barn owl. *J. Neurosci.* **13**, 2837–2852 (1993).
10. Moiseff, A. & Konishi, M. Neuronal and behavioral sensitivity to binaural time differences in the owl. *J. Neurosci.* **1**, 40–48 (1981).
11. Payne, R.S. Acoustic location of prey by barn owls (*Tyto alba*). *J. Exp. Biol.* **54**, 535–573 (1971).
12. Knudsen, E.I. & Konishi, M. Mechanisms of sound localization in the barn owl (*Tyto alba*). *J. Comp. Physiol.* **133**, 13–21 (1979).
13. Olsen, J.F., Knudsen, E.I. & Esterly, S.D. Neural maps of interaural time and intensity differences in the optic tectum of the barn owl. *J. Neurosci.* **9**, 2591–2605 (1989).
14. Keller, C.H., Hartung, K. & Takahashi, T.T. Head-related transfer functions of the barn owl: measurement and neural responses. *Hear. Res.* **118**, 13–34 (1998).
15. Knudsen, E.I., Esterly, S.D. & du Lac, S. Stretched and upside-down maps of auditory space in the optic tectum of blind-reared owls; acoustic basis and behavioral correlates. *J. Neurosci.* **11**, 1727–1747 (1991).
16. Brainard, M.S. & Knudsen, E.I. Sensitive periods for visual calibration of the auditory space map in the barn owl optic tectum. *J. Neurosci.* **18**, 3929–3942 (1998).
17. du Lac, S. & Knudsen, E.I. Neural maps of head movement vector and speed in the optic tectum of the barn owl. *J. Neurophysiol.* **63**, 131–146 (1990).
18. Cai, H., Carney, L.H. & Colburn, H.S. A model for binaural response properties of inferior colliculus neurons. II. A model with interaural time difference-sensitive excitatory and inhibitory inputs and an adaptation mechanism. *J. Acoust. Soc. Am.* **103**, 494–506 (1998).
19. Borisyuk, A., Semple, M.N. & Rinzel, J. Adaptation and inhibition underlie responses to time-varying interaural phase cues in a model of inferior colliculus neurons. *J. Neurophysiol.* **88**, 2134–2146 (2002).
20. Knudsen, E.I. Auditory and visual maps of space in the optic tectum of the owl. *J. Neurosci.* **2**, 1177–1194 (1982).
21. Konishi, M. Coding of auditory space. *Annu. Rev. Neurosci.* **26**, 31–55 (2003).
22. Knudsen, E.I., Blasdel, G.G. & Konishi, M. Sound localization by the barn owl (*Tyto alba*) measured with the search coil technique. *J. Comp. Physiol.* **133**, 1–11 (1979).
23. Gold, J.I. & Knudsen, E.I. Adaptive adjustment of connectivity in the inferior colliculus revealed by focal pharmacological inactivation. *J. Neurophysiol.* **85**, 1575–1584 (2001).
24. Gutfreund, Y. & Knudsen, E.I. Adaptation in the auditory space map of the barn owl. *J. Neurophysiol.* **96**, 813–825 (2006).
25. Knudsen, E.I. & Konishi, M. Center-surround organization of auditory receptive fields in the owl. *Science* **202**, 778–780 (1978).
26. Perrott, D.R. & Musicant, A.D. Minimum auditory movement angle: binaural localization of moving sound sources. *J. Acoust. Soc. Am.* **62**, 1463–1466 (1977).
27. Sheth, B.R., Nijhawan, R. & Shimojo, S. Changing objects lead briefly flashed ones. *Nat. Neurosci.* **3**, 489–495 (2000).
28. Nijhawan, R. Motion extrapolation in catching. *Nature* **370**, 256–257 (1994).
29. Alais, D. & Burr, D. The "Flash-Lag" effect occurs in audition and cross-modally. *Curr. Biol.* **13**, 59–63 (2003).
30. DeBello, W.M. & Knudsen, E.I. Multiple sites of adaptive plasticity in the owl's auditory localization pathway. *J. Neurosci.* **24**, 6853–6861 (2004).